MODELING OF ETHANOL DEHYDRATION BY DIFFUSION DISTILLATION IN CONSIDERATION OF THE SENSIBLE HEAT TRANSFER

Seong Cheol Kim, Dong Woo Lee and Won Hi Hong[†]

Department of Chemical Engineering, Korea Advanced Institute of Science and Technology,
373-1 Kusung-dong, Yusung-ku, Taejon 305-701, Korea

Abstract – The diffusion distillation is the evaporation and diffusion process below the boiling temperature of the mixture in a gap filled with the inert gas. It can separate the azeotropic mixture of ethanol and water. The mass transfer in a differential single column can be described by the Maxwell-Stefan equations. Differential mass balances which can extend a column model from a differential single column to an integral column and heat balances were suggested. The new model considers the sensible heat transfers and develops algorithm which enables to calculate interfacial temperature more precisely at condensing liquid film and include one more iterative loop. The results are compared with the experimental data and other models.

INTRODUCTION

The azeotropic composition of ethanol/water mixture at atmospheric pressure is 0.8934 ethanol mole fraction and is the separation limit in normal distillation. Many processes have been proposed to separate the azeotropic mixture such as azeotropic or extractive distillation, but the third component added should be separated again. The mechanisms of diffusion distillation are as follows [Fullarton and Schlünder, 1983].

The liquid mixture introduced at the top of the column flows down and evaporates at the surface of one plate such as in Fig. 1. The evaporated gas mixture diffuses through an inert gas layer and then condenses at the other plate. The inert gas is used as barrier. Because of the molecular size difference, one component passes preferentially than the other component through stagnant inert gas layer. The temperature of evaporation, the gap width of two plates, and the sort of inert gas influence the degree of separation.

Because of the presence of inert gas, this process is necessarily multicomponent mass transfer system and can be described by the Maxwell-Stefan equations.

The solutions of Maxwell-Stefan equations for a film model can be classified into three groups. The approximate solutions using linearization were obtained by Toor [1964] and Stewart and Prober [1964]. Their solutions rely on the assumption of constancy of the Fick matrix over the diffusion path, and those solutions are not exact when molar concentration is high.

Taylor and Smith [1982] reported explicit solutions. These solutions have a merit of rapidity in calculations, but the results deviate at high molar flux.

The exact solutions with a general matrix method at steady state for isothermal-isobaric diffusion in multicomponent ideal gas mixtures were developed by Krishna and Standart [1976]. Carty and Schrodt [1975] compared the exact solutions with

the results of the approximate solutions and demonstrated the superiority of the exact solutions. Sandall and Dribika [1979] analyzed the experimental results in distillation with the Krishna-Standart method and reported excellent agreements of the results. To improve the robustness of calculation of the mass transfer rate, Taylor and Webb [1981] compared various computational procedures and suggested a new algorithm. Webb and Sardesai [1981] performed experiments for the condensation in vertical tube and discussed the applicability of the several models of multicomponent mass transfer.

On the other hand, other groups performed experiments to separate the azeotropic mixtures in wetted wall column filled with inert gases and described the mass transfer with Maxwell-Stefan equations. Fullarton and Schlünder [1983] concentrated 2-propanol beyond the azeotropic composition of 2-propanol/water mixture and named the process as diffusion distillation. McDowell and Davis [1988] described the process behavior of the diffusion distillation with an integral column model and simulated the experimental data of Fullarton and Schlünder.

In this paper, the results of computer simulation by modified model are compared with that of other models and with the own experimental data.

DESCRIPTION OF DIFFUSION DISTILLATION SYSTEM

Fig. 1 shows a simplified schematic diagram of diffusion distillation. Two concentric tubes consist of wetted-wall column. The feed enters at the top of the column and the condensate and residue are drawn off at the bottom of the column. Ethanol and water mixture flows down the column and some amounts of the mixture are evaporated at the inside surface of the outer tube. Because of different diffusivities in inert gas, water vapor reaches condensation side faster. The mixture of the residue leaving the column can be concentrated beyond the azeotropic composition. Heat loss due to evaporation is supplemented by
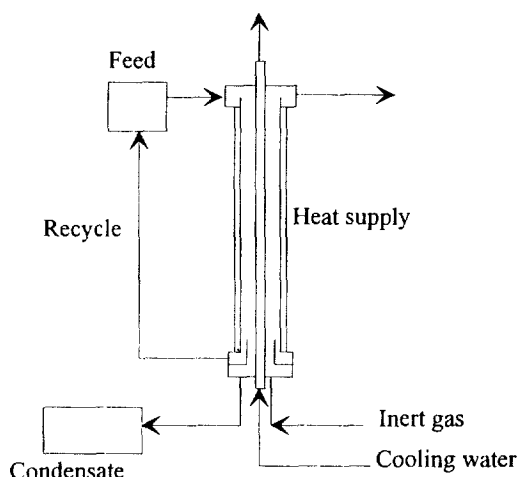
Fig. 1. Schematic diagram of diffusion distillation.

heating of outer wall.

The experiments are carried out with binary ethanol/water mixture at several evaporation side temperatures with different inert gas and annular width. The details of apparatus and experimental conditions are given by Chung et al. [1994].

MODELING OF DIFFUSION DISTILLATION

1. Molecular Diffusion in a Multicomponent System

For ideal mixtures and steady state, and for the unidirectional diffusion under isobaric, isothermal condition, the Maxwell-Stefan equations can be written as follows [Cussler, 1976];

$$\frac{dy_i}{d\eta} = \sum_{\substack{k=1 \\ k \neq i}}^{n} \frac{y_i N_k - y_k N_i}{cD_{ik}/\delta} = \sum_{\substack{k=1 \\ k \neq i}}^{n} \frac{y_i J_k - y_k J_i}{cD_{ik}/\delta} \quad i=1, 2, \cdots, n. \tag{1}$$

The boundary conditions for this equation using film model are

$$\eta = 0 \qquad y_i = y_{ib} \tag{2}$$

$$\eta = 1 \qquad y_i = y_{i\delta} \tag{3}$$

where δ is the film thickness and the dimensionless distance from the bulk gas, η, is defined as $\eta = z/\delta$.

The diffusion flux at bulk gas is given by

$$(J_o) = [B]^{-1} [\Phi] \{\exp[\Phi] - [I]\}^{-1} (y_b - y_\delta) \tag{4}$$

where [I] is the identity matrix.

The matrix [B] is a reciprocal of binary mass transfer coefficients and has elements

$$B_{ii} = \frac{y_i}{k_{in}} + \sum_{\substack{j=1 \\ j \neq i}}^{n} \frac{y_j}{k_{ij}}, \qquad i=1, 2, \cdots, n$$

$$B_{ij} = -y_i \left[\frac{1}{k_{ij}} - \frac{1}{k_{in}} \right]_{i \neq j}, \qquad i, j=1, \cdots, n \tag{5}$$

where $k_{ij} = cD_{ij}/\delta$.

The matrix [Φ] of dimensionless rate factors for multicomponent system is presented as

$$\Phi_{ii} = \frac{N_i}{k_{in}} + \sum_{\substack{j=1 \\ j \neq i}}^{n} \frac{N_j}{k_{ij}}, \qquad i=1, 2, \cdots, n$$

$$\Phi_{ij} = -N_i \left[\frac{1}{k_{ij}} - \frac{1}{k_{in}} \right]_{i \neq j}, \qquad i, j=1, \cdots, n \tag{6}$$

The value of molar flux N_i in stagnant inert gas can be calculated from the molar diffusion flux J_i and bootstrap matrix [β];

$$(N) = [\beta] (J) \tag{7}$$

where the elements of matrix [β] are given by

$$\beta_{ik} = \delta_{ik} + \frac{y_i}{y_n}, \qquad i, k=1, 2, \cdots, n \tag{8}$$

and δ_{ik} is Kronecker delta.

The calculation algorithm of molar flux in multicomponent system using film model has been introduced by Taylor and Webb [1981]. The molar fluxes here are calculated by their algorithm.

To describe mass transfer in diffusion distillation, Fullarton and Schlünder [1983] used the Maxwell-Stefan equation. The compositions of the condensation side can be calculated from the mass balances, vapor-liquid equilibrium, molar flux, and concentration gradient, if the compositions of evaporation side are known. To calculate the concentrations of condensation side, the followings are assumed;

(1) The compositions of the evaporation side do not change along the length of the column.

(2) The annulus is regarded as a plane plate.

(3) The inert gas in the gap remains stagnant and the forced convection does not exist.

(4) The liquid mass transfer resistance in the falling film is negligible.

(5) The liquid and vapor at the interface have their equilibrium compositions.

The constitutive equations are Maxwell-Stefan equations, and the mass transfer coefficients defined here are described by

$$k_{ij} = cD_{ij}/s \tag{9}$$

where s is the gap size between two walls. From assumption (1), Fullarton and Schlünder showed point behavior by solving Eq. (1).

To extend process modeling as an integral column, the differential material balances for the total molar flux must be made [McDowell and Davis, 1988]. For the evaporation side liquid film and condensation side film, the following equations can be written

$$\frac{dL'}{dz} = -N_t \tag{10}$$

$$\frac{dL''}{dz} = N_t \tag{11}$$

where L is perimeter flow rate. Superscripts ' and ", represent the evaporation side and the condensation side respectively.

The component flow and the component molar flux are defined as

$$L_i' = x_i' L' \tag{12}$$

$$\frac{dL_i'}{dz} = -N_i \tag{13}$$

and Eq. (12) can be derived as below

$$\frac{dL_1'}{dz} = x_1' \frac{dL'}{dz} + L' \frac{dx_1'}{dz} \tag{14}$$

From Eq. (13) and (14), the differential change in x_1' is

$$\frac{dx_1'}{dz} = \frac{-1}{L'} \left(N_1 + x_1' \frac{dL'}{dz} \right) \tag{15}$$

and similarly for x_1'' the following equation can be derived

$$\frac{dx_1''}{dz} = \frac{1}{L''} \left(N_1 - x_1'' \frac{dL''}{dz} \right) \tag{16}$$

To calculate the compositions, flow rate, and temperature at each position of the column wall, the following assumptions are also made;

(6) The liquid layer of evaporation side is assumed perfectly mixed across the lateral cross section with respect to composition and temperature.

(7) For the first drop condensed at the top the liquid layer is totally unmixed, implying the infinite mass transfer resistance in the liquid layer, and the liquid layer at all other points along the column is assumed to be well mixed.

The interface temperature of condensation side is calculated from the energy balance. The heat leaving the evaporating interface equals the heat transferred to the condensing interface. If the sensible heat transfer contribution due to mass transfer is neglected, the heat transferred to the condensing interface is described in terms of its latent component only.

The temperature change of evaporation side and coolant is given by

$$L' C_{pL} \frac{dT'}{dz} = Q' - Q'' \tag{17}$$

$$L_c C_{pC} \frac{dT_C}{dz} = Q'', \tag{18}$$

where Q' is the heat input from the outside wall and Q'' is the heat removed from coolant of inner tube. The perimeter flow rates of evaporation side and coolant are denoted by L' and L_c respectively.

The apparatus used in the experiment is a differential single column with recycle but we analyze its results as a long single pass column. If there is a negligible composition change during one passage, then the differential column can be regarded as a series of single column. In addition, if the condensing side temperature and composition effect is negligible, then it is the same as a long single column.

The assumptions made in our modified model [Kim, 1994] are different from the above model in following terms.

For the heat leaving the evaporation side, the conductive heat which carried bodily by the transferring materials are added to the latent heat,

$$Q'' = \sum_{i=1}^{n} H_{vi} N_i + h_y^*(T' - T_I'') \tag{19}$$

where H_{vi} is the heat of vaporization of component i, and h_y^* is the finite flux heat transfer coefficient,

$$h_y^* = h_y \times \frac{\theta}{\exp\theta - 1} \tag{20}$$

and the dimensionless heat transfer rate factor θ [Ackermann, 1973; Colburn and Hougen, 1934] is defined as below

$$\theta = \frac{N_1 C_{pG1} + N_2 C_{pG2}}{h_y}. \tag{21}$$

The heat input from the outside wall is supplied constantly from the outside wall and the temperature of the evaporation side is retained relatively constant at feed temperature. The temperature of the condensation side is obtained from the continuity of heat flux at interface,

$$h_o(T_I'' - T_c) = \sum H_{vi} N_i + h_y^*(T' - T_I''), \tag{22}$$

where h_o is the heat transfer coefficient which includes the heat transfer resistance of the condensed liquid film, wall and coolant. The value of T_I'' cannot be solved directly, but calculated iteratively in order to satisfy Eq. (22).

The flow chart to calculate the interfacial temperature of condensation side is shown in Fig. 2. The differential equations are integrated using the 4th order Runge-Kutta method and equilibrium data are taken from the reference [Gmehling and Onken, 1977].

2. Simulation Condition

To interpret the model, Maxwell-Stefan equation is solved with exact solution which suggested by Taylor and Webb [1981]. To calculate the equilibrium composition of interface, the activity coefficient is estimated from Wilson equation.

The overall heat transfer coefficient, h_o is calculated from the heat transfer in the laminar flow [Bird et al., 1960] and the zero heat transfer coefficient, h_x is from the thermal conductivity of gas/vapor mixture and annular gap. We assume that the heat supplied from the outside wall is constant at all position and the temperature of evaporation side changes along the length of the column.

RESULTS AND DISCUSSION

In order to compare the model performances, we make use of the previous experimental data with air as the inert gas
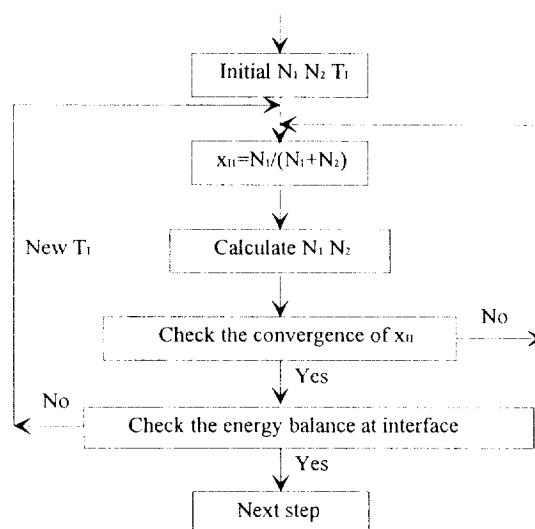

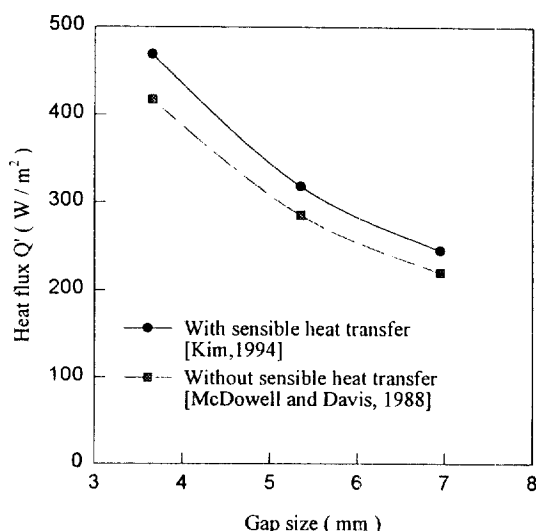Fig. 2. Flow chart for modified energy balance.

Fig. 3. Heat flux required to retain feed temperature 30°C.

Table 1. Ratio of sensible heat transfer to latent heat at different feed temperatures

Feed temperature (°C)	Sensible heat/Latent heat
30	0.1247
40	0.0806
50	0.0451
67	0.0064

Fig. 4. Evaporation side temperature prediction.

[Chung et al., 1994]. Heat supply, evaporation side temperature and composition effects are also tested.

1. Comparison of Heat Requirement

Major difference of the new model from McDowell and Davis model [1988] is explained by Eq. (19). In the new model, the heat transfer at the evaporation side consists of two parts. One is latent heat and the other is sensible heat transfer which allows the consideration of the effect of mass transfer on heat transfer. The model of McDowell and Davis is assumed that the heat transfer due to sensible heat transfer is insignificant. Heat input from outside wall should be chosen to maintain a relatively constant temperature at each points in a column. Then two models need different heat supply to retain feed temperature along the column. As shown in Eq. (19), new model which includes sensible heat transfer requires more heat supply then McDowell and Davis model.

Fig. 3 shows the value of required heat inputs in case of the feed temperature at 30°C for different gap sizes. The ratio of sensible heat to latent heat for each gap sizes is about 10% and so the sensible heat transfer should be calculated.

As the total flux increases, the two values in the right hand side of the Eq. (22) will increase. However it is notable that the first term in that of Eq. (22) could overwhelm the value evaluated with the second term. This might be caused by the fact that the process both including the phase change and mass transfer, the heat required to phase change has dominant effects. Though sensible heat transfer is negligible at high temperature, it gains in importance as the evaporation temperature decreases. The ratio of sensible heat to latent heat for various feed temperatures are presented in Table 1 for the constant gap size of 3.65 mm. Accordingly, sensible heat transfer which take account of mass transfer must be considered when the flux is small.

The value of heat input which used to the new model is applied for the model of McDowell and Davis. The evaporation side temperatures along the column which predicted by two models are shown in Fig. 4. Feed temperature and gap size used in simulations are 40°C and 6.95 mm. As expected, the
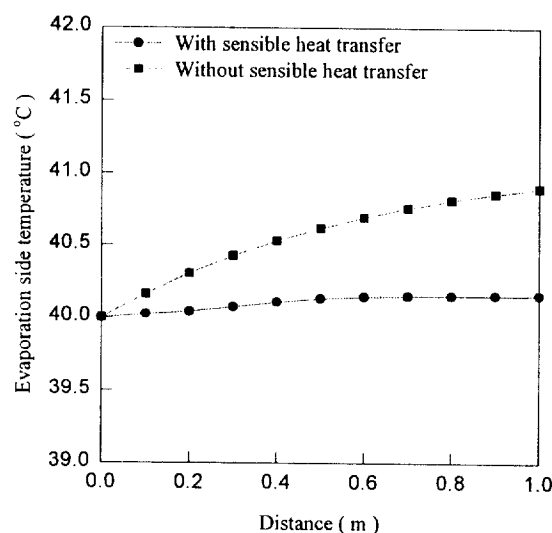
model which does not include sensible heat transfer shows higher temperature at each point of column. The higher temperature prediction in the model of McDowell and Davis causes the higher transferred molar flux in calculation. Along the column, the flow rate of evaporation side decreases in both model and the temperature increases a little. In the experiment, as we supply heat to the outside wall of the column constantly, the temperature of liquid mixture flowing down changes along the column. Therefore, it is necessary to consider the variation of the temperature of liquid mixture in the model.

2. Prediction of Composition and Molar Flux

If heat supply is chosen to maintain the temperature along the column as the temperature of feed, above two models show nearly the same performances in predicting the composition profiles in the column. The molar flux is a function of the vapor compositions of each side and the molar flux affects the composition of condensation side. If the temperatures of each side in two model show little differences, following the assumption (v), two models have the nearly same vapor compositions at interface of both side. And then the condensation side composition, molar flux, and flow rate would have little differences.

In Fig. 5, the experimental data are compared with the values calculated with the Fullarton and Schlünder model [1983], which solves Maxwell-Stefan equation in isothermal condition, and those with the new model. In simulation results, the condensation side composition is represented as below.

$$x_i'' = \frac{N_i}{N_t} \tag{23}$$

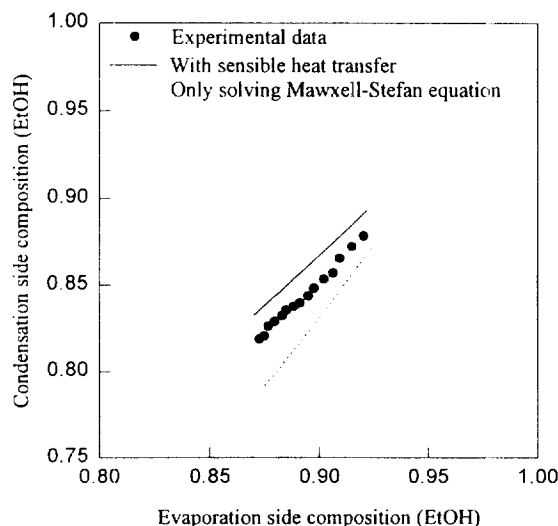The initial temperature of feed entering the column is 40°C
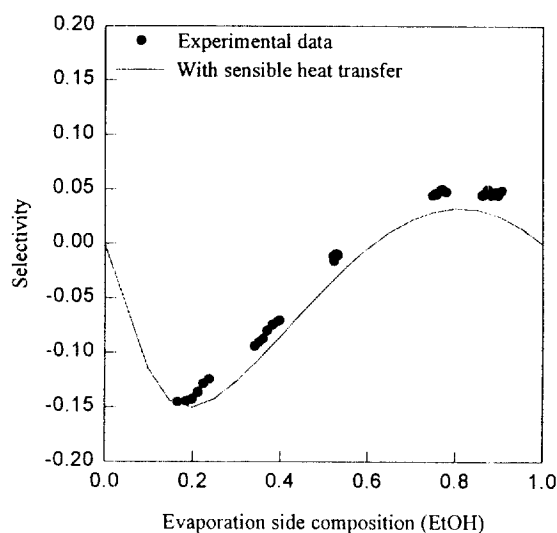
Fig. 5. The comparison of experimental data and models.

Table 2. Selectivities with different feed temperatures

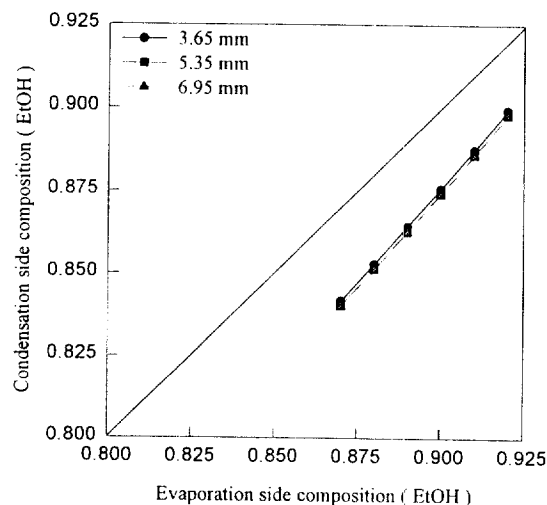| Feed temperature (°C)	S_{exp}	S_{sim}
30	0.0482	0.0323
40	0.0500	0.0372
50	0.0466	0.0368
67	0.0350	0.0219

Fig. 7. Gap size effects on separation.

Fig. 6. Composition effects on separation.

tropic point are shown in Table 2. Maximum selectivity is obtained at 40°C.

Fig. 7 shows the gap size effects. According to the experimental data [Chung et al., 1994], the gap size has an influence only on total flux. Measured experimental value can be affected by free convection and shear stress at falling film [Fullarton and Schlünder, 1983]. At feed temperature 30°C, simulation results show that selectivity increases a little with decreasing gap of both walls. A reason for the different selectivity obtained in simulations are due to interfacial temperature prediction namely evaporating condition. If we do not consider the energy balances, then there would be no difference in selectivity. Because selectivity is determined only by the molecular diffusion which obtained in Eq. (1). But the temperature and composition along the column will be same at all position.

Not only selectivity but also total flux influences the separation. From the condensate flow rate data, we can calculate total flux. The transfer area of wetted wall is calculated using logarithmic-mean diameter.

Since vapor pressures and diffusivities increase with temperatures, the total flux increases also with temperatures. Fig. 8 shows the temperature effect on total molar fluxes at azeotropic composition and Fig. 9 represents the composition effect. The annular gaps are 6.95 and 5.35 mm in each case.

The difference between mass transfer prediction and measurement might be due to the difference in temperature between the simulation and the experiment. The experimental temperature was measured at the outer wall of the tube thus the temperature of the fluid flowing the column is lower than that of the introduced mixture. The other factor for discrepancy may be arisen by the convection. The inert gas introduced can cause convection in the perpendicular direction with diffusion path and then the flux will be decreased.
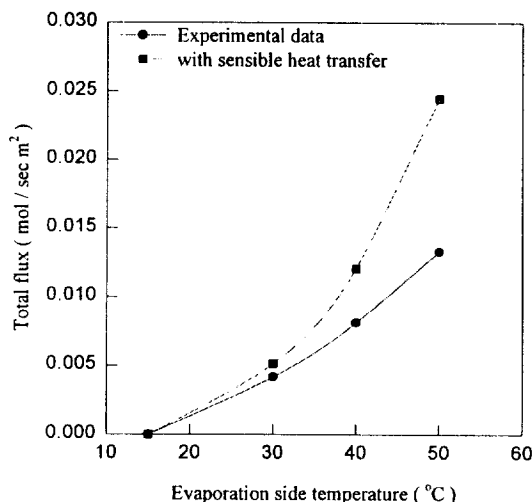
and the gap size of two concentric walls is 6.95 mm. In ethanol/water system, as the prediction of the vapor-liquid equilibrium around the azeotropic point is not correct, it seems that the new model does not have any difference. In IPA/water system or TBA/water system, however, the new model simulates well the experimental data in comparison with only solving the Maxwell-Stefan equation.

The selectivity can be defined as the differences of concentrations between evaporation and condensation side. Because the condensation side composition is determined from the mass transfer of evaporation side, the evaporation side composition affects on the selectivity. Fig. 6 compares the experimental selectivity data with simulation results for the gap size of 5.35 mm. This process is based on both vapor-liquid equilibrium and the diffusivities of each components in the inert gas. Though vapor phase is ethanol rich phase below the azeotropic point, the water diffuses faster and there exists negative selectivity value.

Selectivity is the distance from the diagonal line in Fig. 5. Simulation data with different feed temperatures at the azeo-

Fig. 8. Evaporation side temperature effects on flux.

Fig. 9. Composition effects on total flux.

Fig. 10. Evaporation side composition change with various feed flow rates.
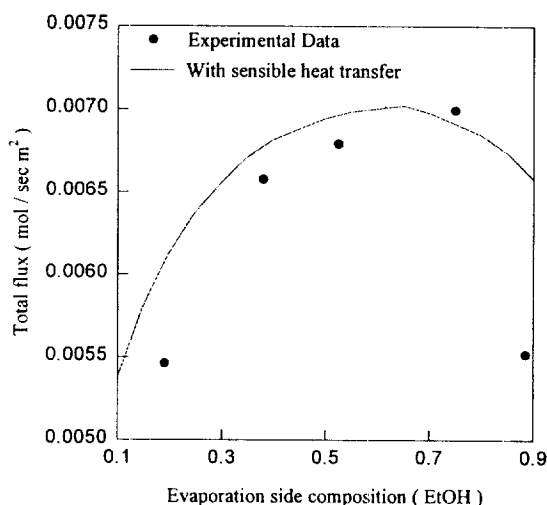
Not only selectivity but also mass transfer is affected by evaporation side composition. The value of total flux has a maximum point at a specific composition in molar bases. In addition, the heat required to evaporate the mixture has the similar trends as shown in Fig. 9. As ethanol concentration is higher, the total mass flux will be higher. But in ethanol rich concentration there is a interval which selectivity does not change. Though flux in mass base increases, the total molar flux decreases. The total flux is determined by the evaporation rate and the diffusion rate. Those two rates govern the mass transfer. As for ethanol, the evaporating rate is faster but the diffusion rate is lower than water.

Differential mass balance accounts for composition change along the column. Fig. 10 represents change in evaporation side composition along the column for 40°C and 6.95 mm gap size. As feed flow rate decreases, enrichment of ethanol increases.

CONCLUSION

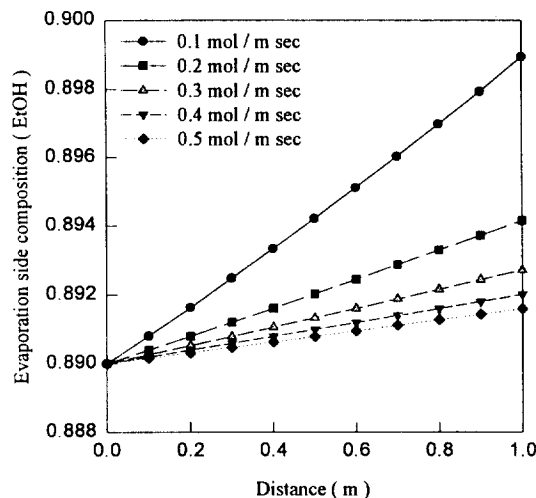The diffusion distillation can separate the azeotropic mixture

of ethanol and water. As demonstrated, diffusion distillation process can be described by the differential mass and heat balances. The temperatures at the interface of both side are calculated using modified heat transfer balance and algorithm which including one more iterative loop. The sensible heat transfer in heat flux is important in case of low temperature of evaporation side but the value can be insignificant when the mass transfers are high. The evaporation side composition effects on the value of total fluxes and selectivities. Because ethanol and water have a different diffusion and evaporation rate, the mixture has a maximum point in mass transfer and has a sign change in selectivity. The heat required to evaporate the mixture also has a maximum. Simulation results are in accord with experimental data. Heat balances which include sensible heat transfer make more realistic boundary layer conditions to determine the total flux and compositions.

NOMENCLATURE

A   : transfer area [m]
[B]   : reciprocal of binary mass transfer coefficient matrix
c   : mixture molar density [mol/m^3]
C_p : heat capacity [J/(kmol °C)]
d_i : inner tube diameter [m]
d_o : outer tube diameter [m]
d_{LM} : log-mean diameter [m]
D   : diffusivity [m^2/s]
h   : heat transfer coefficient [W/(m^{2o}C)]
H   : length of tube [m]
H_v : heat of vaporization [J/kmol]
[I]   : identity matrix
J   : molar diffusion flux [kmol/m^{2}s]
k   : mass transfer coefficient
L   : perimeter flow rate [kmol/(m s)]
N   : molar flux [kmol/(m^{2}s)]
Q   : heat flux [W/m^2]
S   : selectivity
T   : temperature [°C]
x   : liquid mole fraction

y : vapor mole fraction
z : distance along the diffusion path in Eq. (4) vertical distance [m]

Greek Letters

δ : film thickness
δ_{ik} : Kronecker delta
$[\beta]$: bootstrap matrix
$[\Phi]$: dimensionless rate factor
η : dimensionless distance
θ : dimensionless heat transfer rate factor

Subscripts

b : bulk phase
c : coolant
exp : experimental
G : gas phase
i or k : component i or component k
I : interface
L : liquid phase
sim : simulation
t : total

Superscripts

' : evaporation side
" : condensation side
* : finite mass transfer

REFERENCES

Ackermann, G., "Heat Transfer and Molecular Mass Transfer in the Same Field at High Temperatures and Large Partial Pressure Differences", VDI Forschungsh., 8, 1 (1937).

Bird, R. B., Stewart, W. E. and Lightfoot, E. N., "Transport Phenomena", Wiley, New York, 1960.

Carty, R. and Schrodt, J. T., "Concentration Profiles in Ternary Gas Diffusion", Ind. Eng. Chem. Fundam., 14, 276 (1975).

Chung, I. S., Song, K. M., Hong, W. H. and Chang, H. N., "Ethanol Dehydration by Evaporation and Diffusion in an Inert Gas Layer", HWAHAK KONGHAK, 32, 734 (1994).

Colburn, A. P. and Hougen, O. A., "Design of Cooler/Condensers for Mixtures of Vapours with Non-condensing Gases", Ind. Eng. Chem., 25, 1178 (1934).

Cussler, E. L., "Multicomponent Diffusion", Elsevier Scientific Publishing Company, Amsterdam, 1976.

Fullarton, D. and Schlünder, E. U., "Diffusion Distillation: A New Separation Process for Azeotropic Mixtures", Chem. Eng. Fundam., 2, 53 (1983).

Gmehling, J. and Onken, U., "Vapour-Liquid Equilibrium Data Collection Series Vol. 1", DECHEMA, Frankfurt-am-Main, 1977.

Kim, S. C., M. S. Thesis, KAIST, Taejon, Korea (1994).

Krishna, R. and Standart, G. L., "A Multicomponent Film Model Incorporating a General Matrix Method of Solution to the Stefan-Maxwell Equations", AIChE J., 22, 383 (1976).

McDowell, J. K. and Davis, J. F., "A Characterization of Diffusion Distillation for Azeotropic Separation", Ind. Eng. Chem. Res., 27, 2139 (1988).

Sandall, O. and Dribika, M. M., "Simultaneous Heat and Mass Transfer for Multicomponent Distillation in Continuous Contact Equipment", Paper Pres. 3rd Int. Symp. on Distillation, London (1979).

Stewart, W. E. and Prober, R., "Matrix Calculation of Multicomponent Mass Transfer in Isothermal Systems", Ind. Eng. Chem. Fund., 3, 224 (1964).

Taylor, R. and Smith, L. W., "On Some Explicit Approximate Solutions of the Maxwell-Stefan Equations for the Multicomponent Film Model", Chem. Eng. Commun., 14, 361 (1982).

Taylor, R. and Webb, D. R., "Film Models for Multicomponent Mass Transfer; Computational Methods: the Exact Solution of the Maxwell-Stefan Equation", Comput. Chem. Eng., 5, 61 (1981).

Toor, H. L., "Solution of the Linearized Equations of Multicomponent Mass Transfer", AIChE J., 10, 448 (1964).

Webb, D. R. and Saradesai, R. G., "Verification of Multicomponent Mass Transfer Models for Condensation Inside a Vertical Tube", Int. J. Multiphase Flow, 5, 507 (1981).